International Symposium
On Turbulence and Shear Flow
Phenomena (TSFP-9)
June 30 - July 3, 2015 *Melbourne, Australia*

DIRECT NUMERICAL SIMULATION OF THE WAKE OF A NORMAL THIN FLAT PLATE: INFINITE VS. FINITE WIDTH

Arman Hemmati*, **David H. Wood, Robert J. Martinuzzi**
Department of Mechanical and Manufacturing Engineering
University of Calgary, AB, Canada
*ahemmati@ucalgary.ca

ABSTRACT

The wake of a normal thin flat plate of aspect ratio 3.2 was studied using Direct Numerical Simulations at a Reynolds number of 1200 for comparison to the wake of a two-dimensional (2D) plate. Secondary spanwise instabilities, which were responsible for the three distinct flow regimes in the wake of 2D plates, were suppressed by the presence of the shear layers formed at the shorter edges in the three-dimensional (3D) case. There was a unique vortex "peeling" mechanism that detached the vortices in the shear layers on the shorter sides. The peeling mechanism accelerated the shedding process and increased the shedding frequency to 0.317 from 0.154 for 2D plates. It is also associated with increased wake entrainment and a reduction in the mean recirculation length by 40% to $1.6h$. Moreover, the peeling mechanism lead to formation of interlocked vortex loops outside the base region, whose expansion downstream resulted in separation of two counter-rotating vortex structures with respect to the wake centreline. The maximum turbulent kinetic energy along the wake centreline for the 3D case was lower by 76% than in the 2D flow.

INTRODUCTION

The wake of an infinite span (2D) thin flat plate has been investigated using Direct Numerical Simulations (Najjar, 1994; Najjar & Balachandar, 1998; Narasimhamurthy & Andersson, 2009; Hemmati *et al.*, 2015*a*) and Large Eddy Simulations (Joshi, 1994; Hemmati *et al.*, 2015*b*), and experimentally (Fage & Johansen, 1927; Kiya & Matsumura, 1988; Wu *et al.*, 2005). These studies revealed a unique low frequency flow pattern in the wake (Najjar & Balachandar, 1998; Wu *et al.*, 2005; Hemmati *et al.*, 2015*a*). Najjar & Balachandar (1998) and Wu *et al.* (2005) described two flow regimes, *H* and *L*, which were identified by changes in the lift fluctuations and other wake characteristics. Hemmati *et al.* (2015*a*), however, characterized these patterns as three distinct flow regimes, *High, Moderate* and *Low Intensity Shedding*, based on fluctuations in the instantaneous forces, size of the recirculation region, vortex interactions, etc. According to Hemmati *et al.* (2015*a*), regular Karman shedding, *regime M*, was interrupted by a secondary spanwise instability that was identified by a periodic spanwise pressure distribution (Hemmati *et al.*, 2014). During the low intensity shedding, shear layer roll-up was delayed, the recirculation region was elongated, and the pressure drop was reduced across the plate, which lead to lower drag. This was followed by a period of intensified entrainment, during which the roll-up moved closer to the plate, resulting in large lift variations. The proximity of the base vortex to the plate decrease the magnitude of the base pressure and the drag. These regimes featured unique wake structures and vortex interactions identified by vortex dislocation, detachment of streamwise ribs and absence of spanwise rollers. Dislocation of vortices during *Regime L* lead to disappearance of spanwise rollers at $\approx 3h$ downstream the plate. Thus, streamwise ribs were stretched and subsequently detached from their counterpart rollers, which elongated the base region and slowed down the shedding process. Finally, regular shedding was re-established in a short reorganizing period, *Regime M*.

There are very few studies of the wake topology of a finite aspect ratio (3D) thin flat plate. Numerical studies of the behind a thin flat plate have proven difficult using RANS, Detached Eddy and Large Eddy Simulations (Breuer *et al.*, 2003; Hemmati *et al.*, 2015*a*). Experimentally, it is difficult to avoid flow interference in experiments on 3D plates. Aly & Bitsuamlak (2013) provide a rare experimental study. However, there has not been any attempts to identify the unique flow features associated with additional shear layers, vortex interactions and wake dynamics for a 3D plate. Similar studies have been completed for the wake of circular (Roshko, 1961; Bearman, 1968; Okamoto & Sunabashiri, 1992; Williamson, 1996) and rectangular (Lyn *et al.*, 1995; Bailey *et al.*, 2002; Wang *et al.*, 2006, 2009; Bourgeois *et al.*, 2011; Hosseini *et al.*, 2013) cylinders. The downwash effects by the vortices formed on the cylinder free end modified the wake topology from that of an infinite span cylinder (Okamoto & Sunabashiri, 1992; Zdravkovich & Bearman, 1998; Sumner *et al.*, 2004; Wang *et al.*, 2006, 2009; Bourgeois *et al.*, 2011; Hosseini *et al.*, 2013).

This study investigates global flow quantities, i.e. mean pressure, shedding frequency, Reynolds stresses, and the instantaneous forces, as well as vorticity, to identify the deviations from the wake of 2D plates and square cylinders. Simulation setup and computational details are briefly discussed in section 2, which is followed by presentation of results in section 3. Discussions on the result interpretation and comparisons are also included in section 3. Conclusions are listed in the final section.

PROBLEM DESCRIPTION

The flow behind a flat plate of aspect ratio 3.2 was studied using Direct Numerical Simulation (DNS) at $Re = 1200$. A three-dimensional Cartesian co-ordinate system was used with the origin at the plate centroid, the positive $x-$direction aligned with the streamwise flow. The normal, in the direction of the shortest side, and spanwise orientations corresponded with y and $z-$axes, respectively. The infinitely thin plate of height h (in the $y-$direction) and spanwise width (chord) w, is shown in Figure 1 along with the computational domain. The aspect ratio AR was $h/w = 3.2$. The shear layers that occur only in the 3D case will be labeled the "spanwise" shear layers. The domain extended $25h$ in the $x-$ direction and $16h$ in the $y-$ and $z-$directions. The inlet was placed at $5h$ upstream the plate. A,B, C, and D show the four flow monitoring points.

The computational set-up for this study was identical to those of flow past infinite span normal flat plates by Hemmati *et al.* (2015*a*) and Hemmati *et al.* (2015*b*), which, in turn, was designed on the basis of Rodi *et al.* (1997); Najjar (1994); Joshi (1994); Najjar & Vanka (1995); Najjar & Balachandar (1998) and Narasimhamurthy & Andersson (2009). The simulations used 9.3×10^6 hexahedral elements.

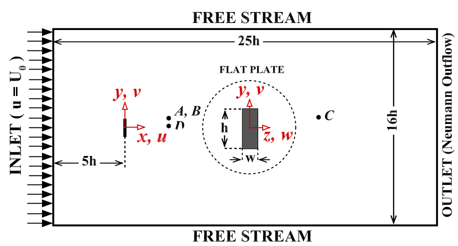

Figure 1: Schematic of the computational domain and the boundary conditions. Location of monitoring points are A:(3,1/2,0), B:(3,1/2,1/2), C:(12,1/2,1/2) and D:(3,0,1/2).

RESULTS & DISCUSSION

Global quantities, such as shedding frequency ($St = fh/U_0$), mean pressure coefficients, mean drag and turbulent kinetic energy (TKE) were used for comparing the wake features. Resolved variables, i.e. profiles of velocity components and Reynolds stresses, were also compared between the two wakes to identify changes in the flow topology and vortex dynamics due to development of additional shear layers on spanwise edges. Shear layer roll-up and vortex detachment processes were identified using contour and iso-surface plots of vorticity and λ_2.

Global flow quantities for the two wakes are presented in Table 1. Vortex shedding intensified with a significant increase in the Strouhal number, $St = 0.317$, compared to the range of St $(0.14 - 0.158)$ reported for the 2D plate at different Re, $250 - 1.5 \times 10^5$ (Hemmati *et al.*, 2015*a*; Narasimhamurthy & Andersson, 2009; Wu *et al.*, 2005; Najjar & Balachandar, 1998; Najjar & Vanka, 1995; Leder, 1991; Kiya & Matsumura, 1988; Fage & Johansen, 1927). Changes in the wake topology and shear layer roll-up processes, which were influenced by presence of additional shear layers, were responsible for the accelerated shedding. The shorter shedding period of the 3D plate coincided with a decrease on the mean drag by 50% in comparison to the 2D plate. Shear layer roll-up and the subsequent vortex detachment was achieved within a shorter distance from the plate, $L_w = 1.6h$, while the recirculation length for a 2D plate was 2.7.

Typical traces of the instantaneous lift coefficient, C_l, and drag, C_d, exhibited more regular shedding behaviour with the force variations being significantly smaller than those of the 2D plate, Figure 2. The three distinct regimes

Table 1: Comparison of the global flow variables in the wake of 3D and 2D thin normal flat plates at $Re = 1200$.

Case	AR	$\overline{C_d}$	St	L_w	Re
3D Plate	3.2	1.16	0.317	1.6	1200
2D Plate (Hemmati *et al.*, 2015*a*)	-	2.13	0.158	2.7	1200
Narasimhamurthy & Andersson (2009)	-	2.31	0.168	1.96	750
Wu *et al.* (2005)	-		0.18		1800
Najjar & Balachandar (1998)	-	2.36	0.161	2.35	250
Najjar & Vanka (1995)	-	2.26	≈0.143	2.55	1000
Leder (1991)	-		0.14	2.5	2.8×10^4
Kiya & Matsumura (1988)	-		0.146		2.3×10^4
Fage & Johansen (1927)	-	2.13			1.5×10^6

observed for the 2D plate, which were identified by changes on the intensity of force variation, do not occur for the 3D plate. The instantaneous behaviour was similar to *Regime M* of a 2D plate, which was previously identified as the regular asymmetric shedding process (Hemmati *et al.*, 2015*a*). Thus, the secondary spanwise instability in the wake of a 2D plate, which have been linked to the three flow regimes (Hemmati *et al.*, 2015*a*, 2014; Najjar & Balachandar, 1998), have been suppressed by the finite spanwise extent of the wake.

One indicator for the secondary spanwise instability was found in the pressure behaviour on the rear surface (Hemmati *et al.*, 2014). Profiles of the pressure coefficients on the $z-$direction of the 2D plate during *Regime H*, Figure 3, illustrate the significance of the secondary instability. Following the magnification of flow irregularities in *Regime H*, shedding cycles retained their regular pattern, *Regime M*. Hemmati *et al.* (2014) further showed that the secondary instabilities initiated during *Regime L* with a large-wavelength spanwise non-linearity in the pressure field. Figure 3 shows that this non-linearity has evolved into a short-wavelength pressure profile. Continuation of this process lead to full suppression of the secondary instability and re-start of regular shedding in *Regime M*. However, pressure field became uniform by bounding the spanwise extent of the shear layers, and thus the wake, using a 3D plate. Hemmati *et al.*

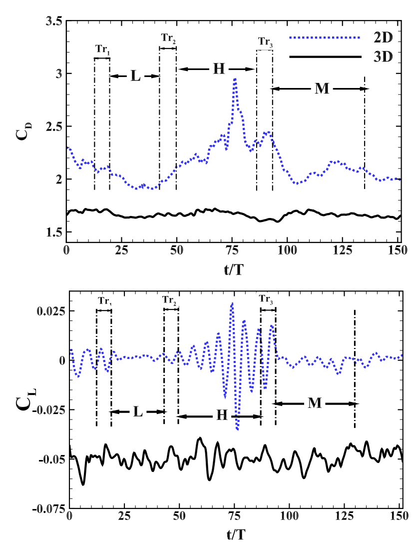

Figure 2: Instantaneous drag (top) and lift (bottom) on 2D (Hemmati *et al.*, 2015*a*) and 3D ($AR = 3.2$) normal thin flat plates at $Re = 1200$.

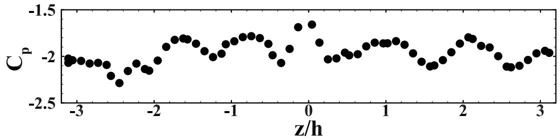

Figure 3: Spanwise distribution of instantaneous pressure coefficients, C_p, on the leeward surface of a 2D normal thin flat plate during *Regime H* (Hemmati *et al.*, 2015*a*) at $Re = 1200$.

(2015*a*) argued that presence of the secondary instabilities during the regular shedding cycles, i.e. asymmetric shedding of *Regime M*, interrupts the regular roll-up and subsequent vortex detachment. The absence of secondary instabilities reduced the vortex generation and detachment length, and subsequently resulted in major changes on the wake topology and vortex dynamics. This lead to a lower drag, compared to a 2D plate. The main re-orientation in the wake, however, was achieved by introducing two additional shear layers.

There are several important observations on the additional shear layers formed on the spanwise edges of the plate. Only a single dominant shedding frequency was obvious in the spectra of the velocity and pressure at points A, B, C and D. This indicates only one dominant shedding cycle in the wake, despite the presence of two sets of shear layers. In other words, the roll-up process for both layers occurred at the same time. This implies that vortex detachment on one edge fixes the entire shedding cycle, while the roll-up of the spanwise vortices was interrupted by a *"peel off"* process. The *peeling* process refers to pre-mature detachment of vortices due to the flow induced by detachment of larger spanwise vortices. Further elaboration on this process are provided later in this section. Moreover, since the shed-

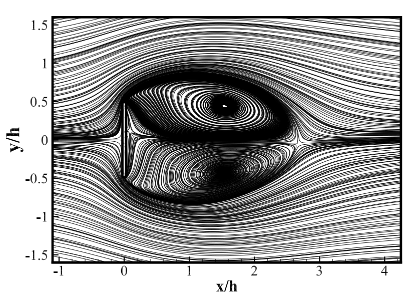

(a) 2D plate (Hemmati *et al.*, 2015*a*)

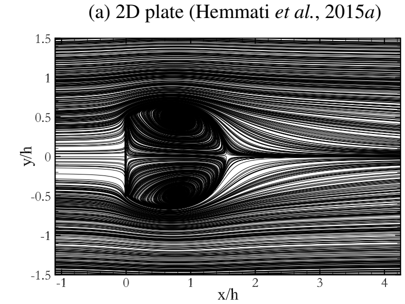

(b) 3D plate ($AR = 3.2$)

Figure 4: Streamline plot of the wake central XY plane for [top] 2D (Hemmati *et al.*, 2015*a*) and [bottom] 3D ($AR = 3.2$) normal thin flat plates at $Re = 1200$.

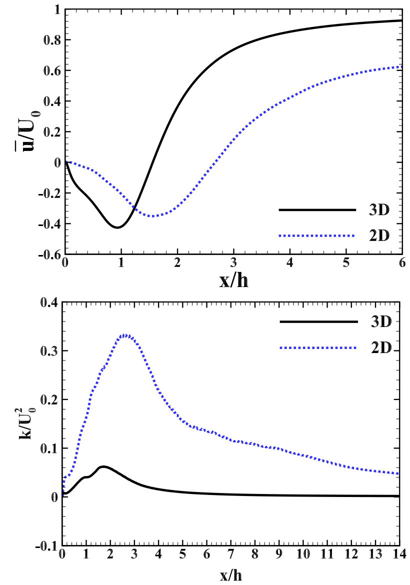

Figure 5: Profile of the mean streamwise velocity, $\overline{u}$, and turbulent kinetic energy, k, along the wake centreline for the flow past 2D (Hemmati *et al.*, 2015*a*) and 3D thin normal flat plates at $Re = 1200$.

ding frequency increased significantly from the 2D plate, the added shear layers have assisted in the vortex shedding process.

Accelerated vortex shedding may be associated with intensified entrainment. Figure 4 shows the streamline plot of the mean velocity field for the 2D and 3D plates. The separating streamline on the 2D plate was 50° in the mean field, which was higher than 30° for the 3D plate. This, in combination with the shorter recirculation length, indicated a greater entrainment angle at the stagnation point for the 3D plate, 64°, relative to the 2D plate, 51°. Moreover, the entrainment velocity, V_E, for the 3D plate was $0.96U_0$, which was significantly larger than $\approx 0.66U_0$ for the 2D plate. The entrainment velocity was approximated using order of magnitude analysis on the entrainment velocity definition, V_E, by Durbin & Reif (2001):

$$V_E = U_0 d_x \delta_{99} - V_{99} \approx O(\frac{T_w}{h_w} U_0) \qquad (1)$$

where T_w is the wake thickness and h_w is the base vortex length. Two-dimensional flow pattern and stronger entrainment are also evident qualitatively by visual inspection of vorticity contours, and quantitatively by looking at distribution of mean streamwise velocity and Reynolds stresses in the wake.

The behaviour of the mean streamwise velocity, $\overline{u}$, along the wake centreline in Figure 5 is typical of the wake evolution, with more reverse flow in the recirculation zone behind the 3D plate, $0.42U_0$. The wake deficit reduced much more rapidly for the 2D plate. With less recirculation and smaller mean velocity gradients, it is not surprising that the 3D wake has lower turbulence levels. As an example, the centreline profile of the turbulence kinetic energy (k) in Figure 5 shows an order of magnitude reduction from the 2D to 3D case. Figure 5 shows a small plateau in k at $x = 0.97h - 1.10h$ which coincides with the *peeling*

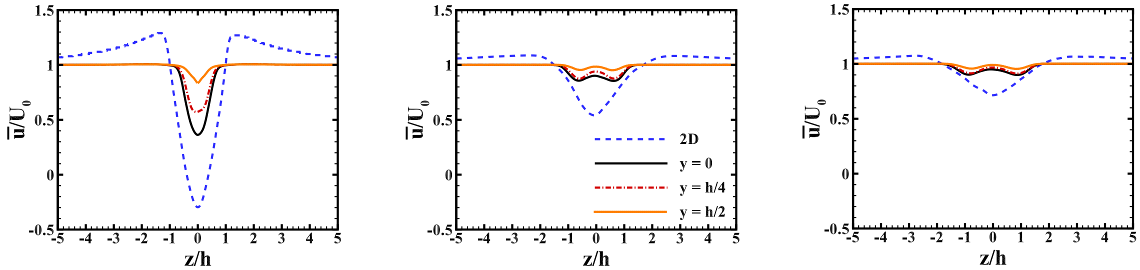

Figure 6: Mean streamwise velocity profiles at$x$ = 2h, 5h and 8h for the wake of a 2D (Hemmati *et al.*, 2015*a*) and 3D ($AR = 3.2$) normal thin flat plate at $Re = 1200$.

off process of the vortices forming on the spanwise edges. After this point, k continued to increase until it reached its maximum value at $x = 1.68h$. Consequently, the wake in proximity to the plate, $x \approx h$, appeared to have all characteristics of a 2D shedding pattern: organized asymmetric roll-up of shear layers, strong reverse flow, single set of vortex-streets, etc. Visual inspection of vorticity contours further confirmed this conclusion. However, the rapid decrease in k outside the recirculation zone coincided with a major change to the flow topology. The mean streamwise velocity at different x, Figure 6, show a double minima in the 2D case. Further, the mean streamwise velocity deficits in the near wake region, outside the base vortex zone, were significantly smaller for the 3D plate. Finally, the normal Reynolds stresses, which are not shown due to space limitations, are roughly equal in this region whereas the $y-$direction normal stress is much larger than the streamwise for 2D flow.

Vortex structures were identified using the λ_2 criteria for the time dependent flow behind 2D and 3D plates with typical examples shown in Figure 7. λ_2 is defined as the second eigenvalue of the $S_{ik}S_{kj} + \Omega_{ik}\Omega_{kj}$ tensor (Jeong & Hussain, 1995), where S_{ij} is the strain rate tensor and Ω_{ij} is the rotation rate tensor. These plots clearly show the *peeling off* process of the smaller vortex structures formed by the spanwise shear layers. Shedding of large scale structures by the roll-up of chordwise shear layers induced streamwise flow away from the plate, which carried out, or *peeled off*, the smaller pre-mature vorteces formed on the adjacent plate edges. Thus, there was a single vortex system detachment from the plate. Asymmetric peeling behind the 3D plate in Figure 7, formed two interlocked vortex-loops, *Stage 1*, at only $5h$ downstream the plate and less than $1.5h$ downstream the base region. First signs of the wake-split also appeared at *Stage 1* of the vortex loop formation in Figure 7. Strong entrainment by the loops on both sides of the wake lead to their expansion farther downstream. These loops were responsible for the wake contraction in the $x,y-$plane (plane of longer edges) and expansion in the $x,z-$plane. Moreover, there were no major wake features in the normal direction, which confirms previous observations. These visualizations, bundled by vorticity contours on the $x,z-$plane, also implied that there exists an inward entrainment, from all directions, feeding the two vortex loops. This is consistent with the flow topology hypothesized by Wang *et al.* (2009) for the quasi-finite square cylinder, in which a horizontal inward flow was induced by the counter-rotating streamwise vortices behind the plate.

Differences in the shear layer roll-up and vortex detachment are responsible for the unique flow topology in the

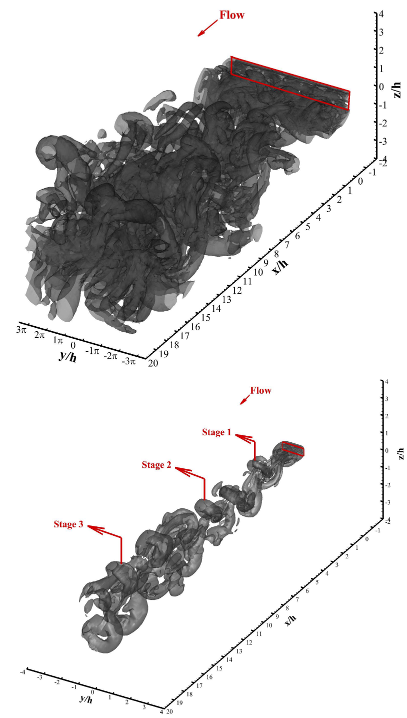

Figure 7: Isosurface plot of $\lambda_2 = 0.1$ in the wake of a 2D (top) and 3D (bottom) normal thin flat plate at $Re = 1200$. The scale is the same in both parts of the figure.

wake of 3D plates. Simultaneous contour plots of vorticity components on both planes are presented in Figure 8 for the 3D plate and in the $x,z-$plane for the 2D plate. One vortex shedding cycle is presented in Figure 8. The roll-up designated A_2 in Figure 8(a) at t_0 was interrupted by formation of a negative vortex at its core, C_2 in Figure 8(a$-t_1$). The opposite rotation of C_2 inside A_2 split the latter vortex at S_2. This phenomenon coincided with the detachment of A_1 in Figure 8(b$-t_2$), which was formed at the other edge. The broken A_2 vortex was carried out by the induced flow of A_1. This is the "*peeling off*" procedure for vortex A_2. Moreover, detachment of A_1 was induced by detachment of vortex C_1 at point S_1 in Figure 8(b). Another important feature of the flow was the vortex dislocation for B_1 at $x = 2.98h$ in Figure 8(b$-t_2$). This phenomenon coincided with formation of the *Stage 1* vortex loop in Figure 7. Furthermore, contour plots of Figure 8(a) confirmed the wake contraction on the plane of dominant height, $x,y-$plane, whereas Figure 8(b) clearly

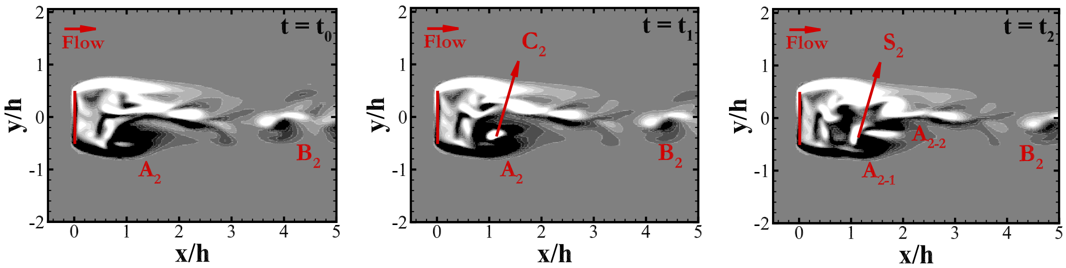

(a) Contour of Ω_z on the XY-Plane for a 3D plate ($AR = 3.2$)

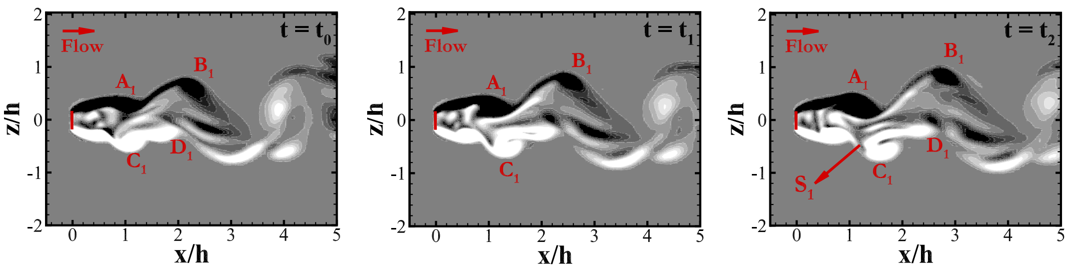

(b) Contour of Ω_y on the XZ-Plane for a 3D plate ($AR = 3.2$)

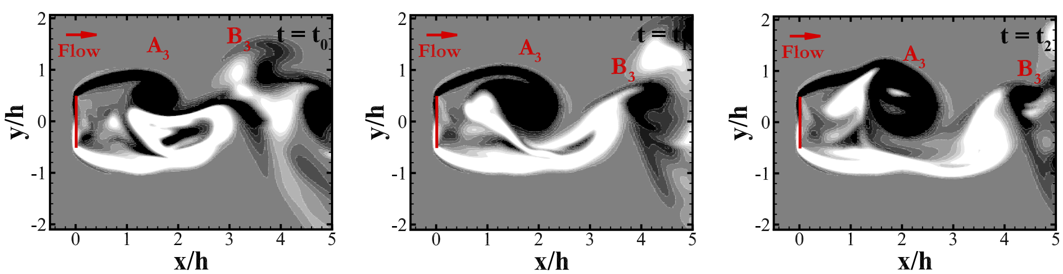

(c) Contour of Ω_z on the XY-Plane for a 2D plate

Figure 8: Contour plots of Ω_z (a, b) and Ω_y (c) at times t_0 (left), t_1 (center) and t_2 (right) in the wake of a 3D ($AR = 3.2$) and 2D normal thin flat plate at $Re = 1200$.

showed a wake expansion due to vortex dislocations on the $x, z-$plane. The asymmetric vortex shedding behind the 2D plate in Figure 8(c) did not include these unique wake features.

Wake structures identified in the vorticity contours, Figure 8, were similar to those of a quasi-finite square cylinder reported by Wang *et al.* (2006, 2009); Bourgeois *et al.* (2011) and Hosseini *et al.* (2013) along the cylinder centreline, $z^* = L/d - 1$. However, small-scale Kelvin−Helmholtz (K−H) vortices formed near the cylinder free end (Okamoto & Sunabashiri, 1992; Wang *et al.*, 2009), corresponding to $y = h/4$ and $y = h/2$ for the plate, were not observed in the flow behind a 3D plate. Moreover, it was shown that the wake of a quasi-finite square (Wang *et al.*, 2006, 2009; Bourgeois *et al.*, 2011; Hosseini *et al.*, 2013) and circular (Zdravkovich & Bearman, 1998; Sumner *et al.*, 2004) cylinder expanded on the plane of cylinder cross-section, i.e. corresponding to the plane of shorter edges in this study, while it contracts inward due to a downwash tip vortex. This behaviour was also observed in the flow behind the 3D plate.

CONCLUSIONS

The wake of a finite aspect ratio (3D) thin flat plate normal to uniform incoming flow was studied by Direct Numerical Simulation and compared to the wake of an infinite span (2D) normal thin flat plate. Aspect ratio of the 3D plate was 3.2 and the *Re* was 1200. This study resulted in the following conclusions:

1. Formation of inward vortex structures, due to the spanwise shear layers, suppressed the secondary spanwise instabilities observed in the wake of 2D plates. Thus, distinct flow regimes identified in the wake of 2D plates, *Regimes H*, *L* and *M*, were eliminated.
2. A single dominant shedding frequency was observed in the wake, which indicated that the two shear layers were rolling up simultaneously at adjacent plate edges. Profiles of mean velocity, Reynolds stresses and turbulence kinetic energy confirmed that vortices were peeled off the chordwise edges by the induced flow resulting from the vortex detachment at the spanwise edges. This mechanism significantly increased the shedding frequency and reduced the recirculation length.

3. Chordwise profiles of the mean streamwise velocity at $2h$, $5h$ and $8h$ downstream the plate deviated significantly from those of the 2D plate. They exhibited strong dependence on the spanwise position and at two and five chords from the plate, all profiles had two minima.
4. Inward vortex structures on the spanwise edges reduced the level of Reynolds stresses (not shown) and the flow organization relative to the 2D plate. Weakening of the spanwise vortices, due to the peeling mechanism, was responsible for the decrease in the Reynolds stresses and the subsequent near equality of the normal stress. Peeling off the pre-mature vortices at the spanwise edges formed an interlocked vortex loop downstream the base region at $x = 3h$. This vortex loop expanded outwards with respect to the $x,y-$plane at $x \geq 5h$. Subsequently, the wake was split with two counter-rotating vortices clearly deviating from the wake centreline. This process was apparent by the double-peek distribution of $\overline{u}$. Following the split, wake contracted in the spanwise direction and expanded simultaneously in the chordwise direction.

ACKNOWLEDGMENTS This study has received support from National Science and Engineering Research Council of Canada (NSERC), Alberta Innovates Technology Future (AITF), ENMAX Corp. and Compute Canada.

REFERENCES

Aly, Aly Mousaad & Bitsuamlak, Girma 2013 Aerodynamics of ground-mounted solar panels: Test model scale effects. *Journal of Wind Engineering and Industrial Aerodynamics* **123, Part A**, 250–260.

Bailey, S. C. C., Martinuzzi, R. J. & Kopp, G. A. 2002 The effects of wall proximity on vortex shedding from a square cylinder: Three-dimensional effects. *Physics of Fluids* **14**, 4160–4177.

Bearman, P. W. 1968 The flow around a circular cylinder in the critical reynolds number regime. NPL Aero Report 1257. NPL.

Bourgeois, J. A., Sattari, P. & Martinuzzi, R. J. 2011 Alternating half-loop shedding in the turbulent wake of a finite surface-mounted square cylinder with a thin boundary layer. *Physics of Fluids* **23** (9), 095–101.

Breuer, M., Jovicic, N. & Mazaev, K. 2003 Comparison of des, rans and les for the separated flow around a flat plate at high incidence. *Int. J. Numr. Meth. Fluids* **41**, 357–388.

Durbin, Paul A & Reif, B. A. Pettersson 2001 *Statistical theory and modeling for turbulent flows*. Chichester; New York: Wiley.

Fage, A. & Johansen, F. C. 1927 On the flow of air behind an inclined flat plate of infinite span. *Proceedings of the Royal Society of London. Series A, Containing Papers of a Mathematical and Physical Character* **116** (773), 170–197.

Hemmati, A., Wood, D. H. & Martinuzzi, R. J. 2014 Wake dynamics behind a normal thin flat plate at moderate reynolds numbers. In *Progress in Turbulence VI*. Springer.

Hemmati, A., Wood, D. H. & Martinuzzi, R. J. 2015*a* Characteristics of distinct flow regimes in the wake of an infinitely span normal thin flat plate. *International Journal of Heat and Fluid Flow.* (In Preparation).

Hemmati, A., Wood, D. H. & Martinuzzi, R. J. 2015*b* On modeling of flow past normal thin flat plates. *In Preparation* .

Hosseini, Z., Bourgeois, J. A. & Martinuzzi, R. J. 2013 Large-scale structures in dipole and quadrupole wakes of a wall-mounted finite rectangular cylinder. *Experiments in Fluids* **54** (9), 1–16.

Jeong, Jinhee & Hussain, Fazle 1995 On the identification of a vortex. *Journal of Fluid Mechanics* **285**, 69–94.

Joshi, Dhananjay Shamrao 1994 Numerical studies of the wake of a plate normal to a free stream. PhD thesis, University of Illinois at Urbana-Champaign, USA.

Kiya, M. & Matsumura, M. 1988 Incoherent turbulence structure in the near wake of a normal plate. *Journal of Fluid Mechanics* **190**, 343–356.

Leder, A. 1991 Dynamics of fluid mixing in separated flows. *Physics of Fluids A* **3** (7), 1741–1748.

Lyn, D. A., Einav, S., Rodi, W. & Park, J.-H. 1995 A laser-doppler velocimetry study of ensemble-averaged characteristics of the turbulent near wake of a square cylinder. *Journal of Fluid Mechanics* **304**, 285–319.

Najjar, F.m. & Vanka, S.p. 1995 Effects of intrinsic three-dimensioanlity on the drag characteristics of a normal flat plate. *Physics of Fluids* **7** (10), 2516.

Najjar, Fady Michel 1994 Direct numerical simulation of separated and separated-reattaching flows on massively parallel processing computers. PhD thesis, University of Illinois at Urbana-Champaign, USA.

Najjar, F. M. & Balachandar, S. 1998 Low-frequency unsteadiness in the wake of a normal flat plate. *Journal of Fluid Mechanics* **370**, 101–147.

Narasimhamurthy, Vagesh D. & Andersson, Helge I. 2009 Numerical simulation of the turbulent wake behind a normal flat plate. *International Journal of Heat and Fluid Flow* **30** (6), 1037–1043.

Okamoto, Shiki & Sunabashiri, Yukisada 1992 Vortex shedding from a circular cylinder of finite length placed on a ground plane. *Journal of Fluids Engineering* **114** (4), 512–521.

Rodi, W., Ferziger, J. H., Breuer, M. & Pourquie, M. 1997 Status of large eddy simulation: Results of a workshop. *Journal of Fluids Engineering* **119** (2), 248–262.

Roshko, A. 1961 Experiments on the flow past a circular cylinder at very high reynolds number. *Journal of Fluid Mechanics* **10**, 345–356.

Sumner, D., Heseltine, J. L. & Dansereau, O. J. P. 2004 Wake structure of a finite circular cylinder of small aspect ratio. *Experiments in Fluids* **37** (5), 720–730.

Wang, H, Zhou, Y, Chan, C & Zhou, T 2009 Momentum and heat transport in a finite-length cylinder wake. *Experiments in Fluids* **46** (6), 1173–1185.

Wang, H. F., Zhou, Y., Chan, C. K. & Lam, K. S. 2006 Effect of initial conditions on interaction between a boundary layer and a wall-mounted finite-length-cylinder wake. *Physics of Fluids (1994-present)* **18** (6), 065106.

Williamson, C. H. K. 1996 Three-dimensional wake transition. *Journal of Fluid Mechanics* **328**, 345–407.

Wu, S. J., Miau, J. J., Hu, C. C. & Chou, J. H. 2005 On low-frequency modulations and three-dimensionality in vortex shedding behind a normal plate. *Journal of Fluid Mechanics* **526**, 117–146.

Zdravkovich, M. M. & Bearman, P. W. 1998 Flow Around Circular CylindersVolume 1: Fundamentals. *Journal of Fluids Engineering* **120** (1), 216–216.